

1 ***Characterisation of aeolian sediment accumulation and preservation***
2 ***across complex topography***

3
4 Alex S Hay¹, D. Mark Powell¹, Andrew S Carr^{1*}, Ian Livingstone².

5
6 ¹School of Geography, Geology and the Environment, University of Leicester, University Road,
7 Leicester, LE1 7RH, UK

8
9 ² The Graduate School, University of Northampton, Northampton, NN2 7AL, UK

10
11
12
13 *Corresponding author: asc18@le.ac.uk +44 116 252 3851

Abstract

14

15 Topography fundamentally influences the distribution and morphology of aeolian landforms via the
16 modification of surface wind flow and the creation of space for sediment deposition. This has been
17 observed at both landform (individual topographic dune forms) and macro-landscape (sand sea)
18 scales. Although previous studies have considered several effects of topography on aeolian
19 landforms, the patterns of landscape-scale aeolian sediment accumulation that emerge at the meso-
20 scale, within topographically complex environments have received less consideration.

21 To address this, we present an approach that combines information on the presence of surficial sand
22 (via remote sensing) with the morphometric feature classification method, LandSerf. Using the Cady
23 Mountains in the Mojave Desert as a case study, we explore the relationships between sand cover
24 and topographic indices over length scales of 10^2 - 10^3 m. Field observations are then used to refine
25 our understanding of these patterns.

26 Aeolian deposits across the Cady Mountains are strongly controlled by the topography. Although
27 sand cover is often continuous and highly variable in depth, four archetypal “accommodation space
28 types” are identified from the morphometric analysis: Slopes, Plains, Valley-Fills, and Slope-Valley
29 composite. Specific aeolian landforms within these accommodation spaces may manifest as sand
30 ramps and climbing and falling dunes, particularly on mountain front Slopes, and sand sheets on
31 downwind Plains within the mountain block. In areas of high sediment supply, these may also
32 coalesce, as exemplified by the extensive and compositionally complex Slope-Valley composites
33 in the northern Cady Mountains.

34 In conjunction with field observations, we argue that topography, moderated by proximity to
35 sediment supply, strongly influences the character of the aeolian sedimentary record. However, even
36 within the relatively complex landscape studied here, 90% of the mapped sand accumulation is
37 associated with the four identified accommodation space types identified. The implication is that
38 areas of such complex topography are amenable to analysis within the scheme outlined and that
39 this can potentially be used to interpret the accompanying dune chronologies.

40 **Keywords:** LandSerf, Mojave Desert, sand ramp, climbing dune, DEM

41

42 **Research highlights:**

- 43 • First attempt to analyse large-scale patterns of aeolian sediment accumulation within
44 complex topography
- 45 • Combined remote sensing-morphometric analysis of aeolian sand-topography relations
- 46 • Three accommodation space types one composite type account for majority of sand
47 occurrence
- 48 • Aeolian preservation at any locale is contingent on topography and sediment supply

49 **1. Introduction**

50 Topography is a fundamental control on the transportation and deposition of aeolian
51 sediment across a range of spatial scales. At the macro-scale (tens to hundreds of kilometers),
52 topography influences the distribution of sand seas (e.g. Wilson, 1973), as well as the strings of dune
53 fields that develop within aeolian sediment transport pathways steered by macro-scale landscape
54 structures. Well-known examples of the latter occur in the Basin and Range landscapes of the
55 southwest USA (Zimbelman *et al.*, 1995; Kocurek and Lancaster, 1999; Muhs *et al.*, 2017).
56 Topography also controls the distribution and form of individual landforms at the micro scale (metres
57 to tens of metres), as obstacles and vegetation induce local wind deceleration, acceleration,
58 deflection and blocking (Howard, 1985; Hesse, 2019). Several types of topographically controlled
59 dune form result. Sand transported onto the windward face of an obstacle can form a climbing dune
60 (White and Tsoar, 1998; Lui *et al.*, 1999; Dong *et al.* 2018) or, if the windward face of the obstacle is
61 steeper than $\sim 50^\circ$, an echo dune (Tsoar, 1983; Lui *et al.*, 1999; Clemmensen *et al.*, 1997; Qian *et al.*,
62 2011). Falling dunes form on lee slopes of obstacles (Ellwein *et al.*, 2015), while lee dunes develop
63 downwind of gaps between obstacles (e.g. Xiao *et al.*, 2015).

64 At intermediate (meso) scales – hundreds of metres to several kilometres – aeolian sands
65 may coalesce against mountain fronts forming sand ramps (Lancaster and Tchakarian, 1996;
66 Bertram, 2003; Rowell *et al.*, 2018a). In regions of high desert relief and topographic complexity,
67 wider swathes of the landscape can also be variably draped in sand (e.g. Dong *et al.*, 2018) producing
68 an array of individual bedforms, as well as more subtle, coalesced or composite aeolian landforms.
69 In South Africa, for example, Telfer *et al.* (2014) observed that although well-defined sand ramps
70 occurred against larger mountains, a less easily delineated aeolian sediment cover mantled much of
71 the landscape, rather like a coversand (e.g. Kocurek and Nielson, 1986). In other studies, valleys
72 have been identified as influencing both upwind and downwind wind velocity and turbulence
73 (Bullard and Nash, 2000; Bourke *et al.*, 2004; Garvey *et al.*, 2005; Ellwein *et al.*, 2011; 2015). Ellwein
74 *et al.* (2015) observed that valley topography also traps aeolian sand, variously forming falling dunes,
75 pairs of falling and climbing dunes, or in locales where sediment supply is high, coalesced “eolian
76 valley-fills”. Thus at the meso-scale we might anticipate that adjacent, repeated and nested aeolian
77 deposits can develop, with sand occurrence and thicknesses varying significantly in response to
78 topographically-induced changes in wind direction and velocity. The valley fill examples above
79 illustrate that topography also provides the space for aeolian sand to accumulate. The term

80 'accommodation space' describes locales where aeolian sediment transport capacity is reduced and
81 net sediment accumulation occurs. Topography frequently presents such opportunities and in this
82 respect can be considered as a fundamental control influencing sand accumulation from the micro
83 (e.g. Ventra et al., 2017) to the macro (e.g. Dong et al., 2018) scales.

84 At meso scales and over long timescales (e.g. $10^2 - 10^5$ years) the location and availability of
85 accommodation spaces will vary in response to changing wind regime or the effectiveness of
86 processes opposing aeolian landform development and preservation. The latter are governed by the
87 underlying topography including, for example, overland flow (Ventra *et al.*, 2017). Furthermore,
88 aeolian landforms that partially or completely fill their accommodation spaces (e.g. Bateman *et al.*,
89 2012; Rowell *et al.*, 2018a) effectively become the topography and will in turn alter the operation of
90 other processes, such as the potential to generate surface run off (Ellwein *et al.*, 2015).

91 The state of an aeolian sediment accommodation space is thus conceived as emerging from
92 the continuous interaction between wind flow, topography and the balance between sediment
93 supply and competing erosive processes. The latter factors are sensitive to wider climate change,
94 while erosive processes themselves are also influenced by topography. We can anticipate that the
95 changing balance of these factors will lead to the repeated formation, reworking, destruction of
96 aeolian landforms (Ventra *et al.* 2017). Thus, when using topographically controlled dunes as
97 palaeoenvironmental archives (e.g. Bateman *et al.*, 2012; Rowell, *et al.*, 2018b; Paichoon, 2020;
98 Schaetzel *et al.*, 2020), or in more general interpretations of the aeolian geomorphic history, an
99 understanding of the dynamic creation and preservation constraints imposed by topography is
100 required.

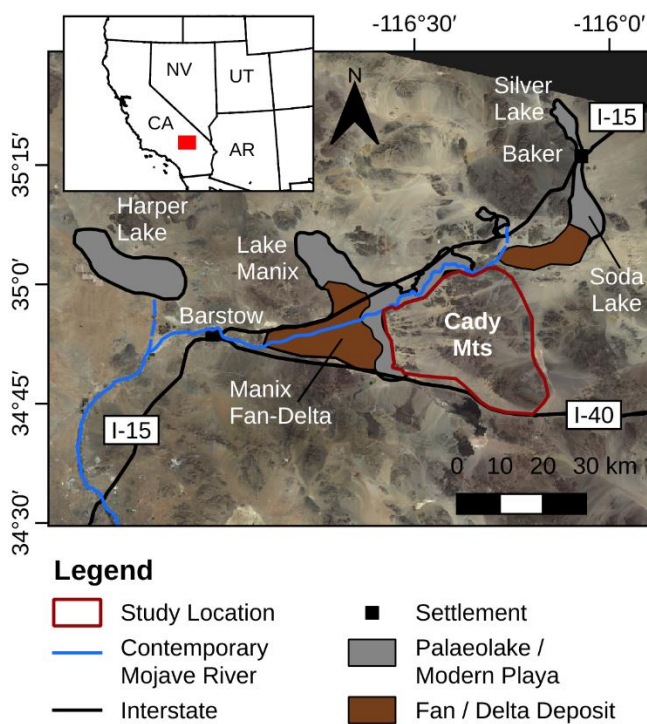
101 This study considers how we achieve an understanding of such potentially complex
102 scenarios, beginning with a more general question and aim: how can we characterise and
103 understand the meso scale (10^2 - 10^3 m) patterns of aeolian sediment accumulation within
104 landscapes of topographic complexity? To address this we sought to develop a novel approach that
105 considers how the character of a variable and partly continuous distribution of aeolian sand can be
106 related in a semi-quantitative manner to the underlying topography. We applied an automated
107 morphometric feature classification method – the LandSerf GIS (Wood 1996) – to a high relief,
108 topographically complex desert landscape, which we then combined with remote sensing-derived
109 sand cover distributions. The relationship between the distribution of sand cover and topography,
110 as represented by morphometric feature class, was established by combining these datasets, and

111 the resulting outputs were further integrated with field observations. This approach allowed us to
112 consider the occurrence of sand in relation to landscape form and in the context of existing
113 classifications of meso-scale topographic dune forms.

114 2. Methodology

115 2.1 Regional Setting

116 The Mojave Desert, California, is characterised by broad, flat basins separated by mountainous
117 topography. It is a region in which the role of topography in shaping aeolian geomorphology is long
118 recognised, with some basins identified as source-to-sink aeolian transport corridors flanked by
119 topographic dunes (Evans, 1962; Smith, 1984; Lancaster and Tchakerian, 1996). The emplacement
120 timings, morphologies (e.g. Lancaster, 1994; Tchakerian, 1991; Clarke and Rendell, 1998) and
121 sediment sources (Kocurek and Lancaster, 1999; Ramsey *et al.*, 1999; Pease and Tchakerian, 2003;
122 Muhs *et al.*, 2017) of some of these dunes have been investigated, and the importance of aeolian-
123 fluvial-lacustrine interactions highlighted (Lancaster and Tchakerian, 2003). The Pleistocene
124 palaeoenvironmental history of the region is also well-studied. Although the contemporary climate
125 is semi-arid, it was markedly cooler and wetter during the Late Pleistocene, resulting in perennial
126 flow of the Mojave River and the maintenance of several palaeo-lake systems (*inter alia*; Wells *et al.*,
127 2003; Enzel *et al.*, 2003).



128

129 **Figure 1:** Location map and satellite image for the Cady Mountains, within the southwest USA,
130 showing the location of the Cady Mountain Block in relation to the Mojave River, palaeo-Lake Manix,
131 Soda and Silver Lakes, which in the past formed palaeo-Lake Mojave, as well as Harper Lake Basin.
132 Also shown is the approximate location of the Lake Manix fan delta, a putative source for the Cady
133 Mountains aeolian deposits.

134

135 The Cady Mountains (**Figure 1**) provide our case study for a region of complex topography
136 within a landscape associated with recent and Pleistocene aeolian activity (Smith, 1984; Zimbelman
137 *et al.*, 1995; Laity, 1992). Today the area experiences a semi-arid climate, with cool winters and warm
138 summers. Mean annual precipitation is ≤ 150 mm yr⁻¹ and annual evaporation is around 2000 mm
139 yr⁻¹ (Blaney 1957; Enzel, 1992; Muhs *et al.* 2017). Precipitation is associated with cool season frontal
140 systems (approximately 60 % of rainfall) or summer convective systems (approximately 40 % of
141 rainfall (Hay, 2018)). Winds, particularly those of sufficient velocities to transport sand, are
142 dominantly from the west, with subordinate northerly and southerly winds associated with the
143 winter and summer (Laity, 1992; Muhs *et al.*, 2017).

144 The Cady Mountains are located 50 km east of Barstow and form a mountain block ~ 25 km x
145 ~ 35 km that lies on the southern and eastern margins of (palaeo) Lake Manix (**Figure 1**). It has been
146 proposed that the former lake sediments of the Manix Basin, notably those upwind of the Cady
147 Mountains in the Manix Fan-Delta area, became available for transportation into the Cady
148 Mountains via westerly winds after Lake Manix drained ~ 25 ka (Meek, 1989; Reheis and Redwine,
149 2008; Laity 1992; Bateman *et al.*, 2012). Such inferences are in part based on studies of the sand
150 ramp at Soldier Mountain, which lies on the northwest corner of the Cady Mountains (Lancaster and
151 Tchakarian, 1996; Rendell and Sheffer, 1996; Bateman *et al.*, 2012). The widespread occurrence of
152 surficial sands and ventifacts (Laity, 1992) on the windward (western) side of the Cady Mountains,
153 as well as the potential constraints on past changes in sediment availability inferred from the
154 draining of Lake Manix, allow us use this locale as a case study to explore the patterns of aeolian
155 sediment emplacement across a complex landscape.

156 **2.2 Remote sensing of sand cover distribution**

157 A cloud-free Landsat 8 image was acquired by the USGS (via <http://earthexplorer.usgs.gov>) on 27th
158 September 2013 at 18:24 GMT. The spectral influence of vegetation is insignificant (Hay, 2018). A 30
159 m-resolution land cover classification was obtained in ERDAS Imagine 2013 using the Eolian Mapping
160 Index (EMI) (Khiry, 2007) as a false-colour composite (for details see Hay, 2018). This classification

161 distinguished the principal land cover types: (1) Sand Cover, (2) Stone-Covered Sands, (3) Rock
162 Surfaces and (4) Other Land Covers (0.1% of image, principally vegetation). Capitalisation of these
163 terms henceforth signifies reference to the classification outputs. Reference data, acquired via field
164 survey, geotagged photographs and detailed Google Earth imagery, were used as training data (46
165 areas each of at least 50 pixels) for the classifier and for accuracy assessment (an Error Matrix
166 verified with reference land cover at 267 points). To allow for the location error on the Global
167 Navigation Satellite System (GNSS) (approximately 30 m), the reference data and land cover
168 classification were considered to agree if the reference data at each location matched more than
169 half of the pixels within a 3x3 window centred on that location. The classified image had an overall
170 accuracy of 87%. The “Other Land Covers” class was removed from subsequent analyses as it
171 accounted for a negligible proportion (0.1%) of the image and was mostly present as an area of high
172 elevation vegetation. Field observations confirmed that the Sand Cover and Stone-Covered Sand
173 classes represent accumulated sediment surfaces, and that the latter largely comprises a lag surface
174 (pavement) of clasts overlying deposits volumetrically dominated by sands (**Figure S1**). The Rock
175 Surface class represents unmodified topography comprising largely un-weathered bedrock
176 sometimes covered by a thin mantle of weathered material.

177

178 **2.3 Mapping surface morphometry**

179 **2.3.1 Data sources and processing**

180 The Digital Elevation Model (DEM) obtained from the USGS National Elevation Dataset
181 (<https://nationalmap.gov/elevation.html>) was sub-setted and re-sampled to the same coverage,
182 spatial reference and spatial resolution (30 m) as the Landsat 8 image. This was defined to include
183 the Cady Mountains, but not the Mojave River, adjacent playa surfaces or areas of human influence
184 (**Figure 1**).

185

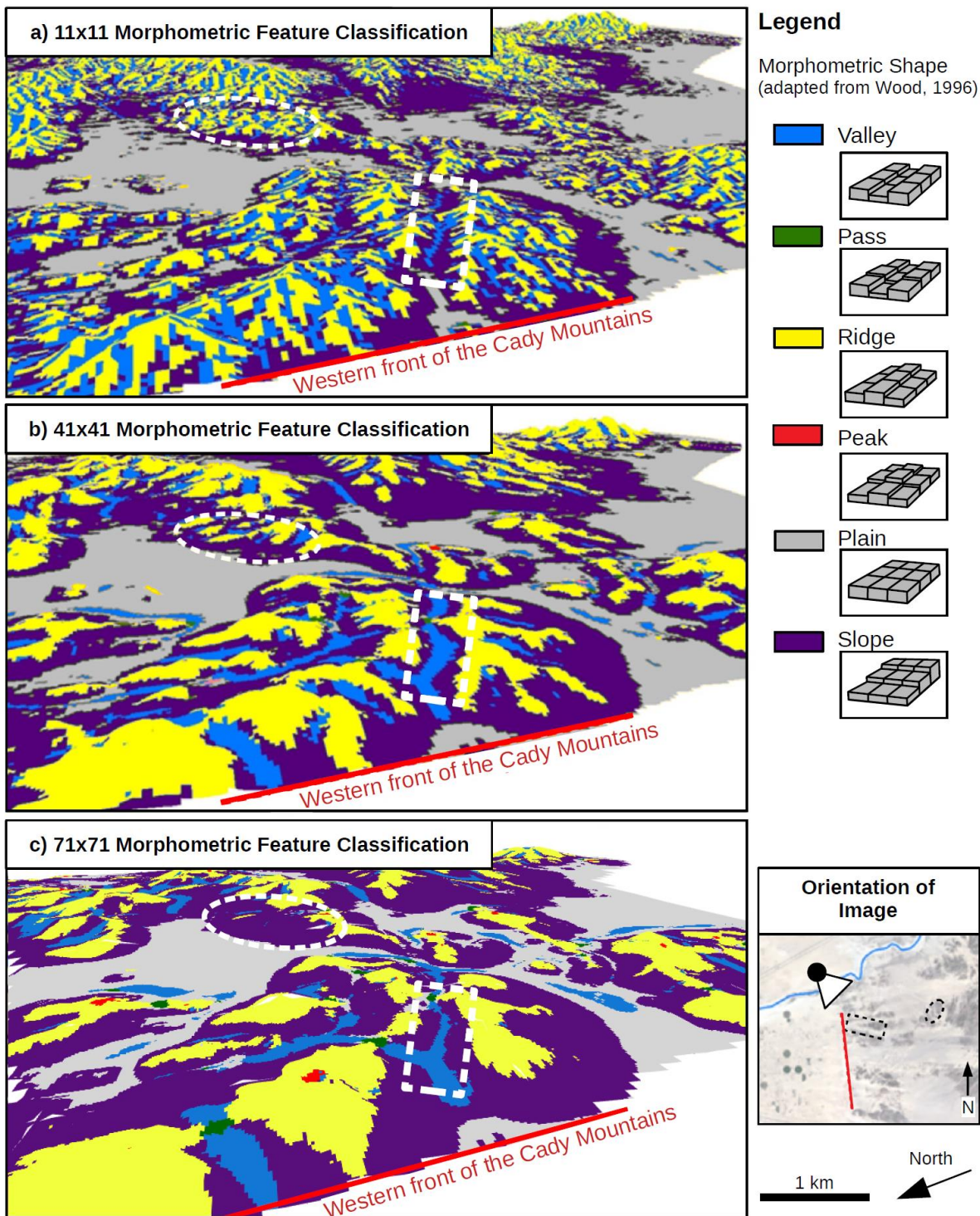
186 **2.3.2 Morphometric parameter determination**

187 LandSerf was used to classify the landscape morphometry following Wood (1996, 2009a; 2009b).
188 Morphometric analysis of the DEM rests on comparing each pixel with those adjacent to it using a
189 user-selected grid (e.g. the parameter slope is derived from elevation change across a three-by-three
190 grid). The size of the grid from which morphometric parameters are obtained, termed the “window-

191 size”, can be varied with the scale of analysis required. This recognises that both morphometric
192 parameters and features are scale-dependent and nested within the landscape (see Wood, 1996;
193 Fisher *et al.*, 2004; Drăguț and Eisank, 2011).

194 The LandSerf feature classification is established using a bi-quadratic polynomial
195 approximation of the surface across a specified range of window sizes and is achieved by establishing
196 the rate of change of three orthogonal components (plan curvature, profile curvature and slope)
197 (Wood, 1996; 2009a; 2009b). LandSerf then classifies the landscape into six morphometric classes;
198 Passes, Peaks, Plains, Ridges, Slopes and Valleys (**Figure 2**). As with the land cover classification we
199 henceforth capitalise these terms to clarify when we are referring to LandSerf-derived
200 morphometric classes. The Plain morphometric class is reserved for flat or undulating surfaces
201 lacking significant hills or depressions and needs to be distinguished from the Slope class (e.g.
202 hillslopes or piedmont features that have a non-zero slope). As very few areas have slope gradients
203 and plan or profile curvatures of exactly zero, a threshold of 2° slope gradient is used to distinguish
204 between Plain and Slope. A gradient threshold is also used to define how steep a surface must be to
205 be considered part of a Pass or Peak and then a slope curvature threshold – a dimensionless ratio
206 that defines the concavity or convexity of a part of the landscape – is used to separate these classes
207 (Wood, 1996; 2009a). These slope and slope curvature thresholds were set at 1° and 0.1 respectively
208 and peaks were only classified as such where they had a relative drop to surrounding topography of
209 more than 50 m.

210 The morphometry parameter slope was calculated as a continuous variable across the raster
211 dataset but is shown as a series of classes that represent areas of shallow (2-6°), intermediate (6-
212 11°) and steep (>11°) slopes (adapted from Miliareisis, 2001; Norini *et al.*, 2016). Aspect was treated
213 similarly but was presented using 16 classes of equal width. We also defined valley orientation using
214 the long-axis azimuth of the valley floor as identified by clusters of valley pixels with a spatial extent
215 greater than 0.5 km² (six pixels).



216

217 **Figure 2:** Outputs of the LandSerf analyses of the Cady Mountains presented as southeast looking
 218 oblique views of the northwest of the Cady Mountain Block. The three panes (a-c) show the
 219 morphometric classification for the same portion of landscape at three examples of analysis scales
 220 (i.e. different maximum window size ranges): a) 3x3 to 11x11 pixels; b) 3x3 to 41x41 pixels; 3x3 to
 221 71x71 pixels. Each pixel in image the represents the most common morphometric class at the range
 222 of scales considered. The legend illustrates the six morphometric classes. The lower right-hand image
 223 shows the direction of view with an image of the study area, with the Mojave River in blue and the
 224 Western Flank of Cady Mountains shown in red.

225 **3. Results**

226 **3.1 Sensitivity to the scale of analysis**

227 LandSerf undertakes multi-scale morphometric analyses by averaging results over a range of
228 window-sizes (Wood, 1996). However, unless one is seeking to undertake an explicit multi-scale
229 analysis, the choice of window size range used for the final morphometric classification must be
230 commensurate with the scale of interest. This study is primarily concerned with the influence of the
231 meso-scale mountain topography on patterns of aeolian sediment accumulation, which we
232 anticipated to span length scales of the order 10^2 to 10^3 m. The effect of varying the LandSerf window
233 size was therefore analysed by considering classifications derived from a range of different maximum
234 window sizes, ranging from 11x11 to 81 x 81 pixels (**Table 1 and Figure 2**). Larger window sizes tend
235 to smooth the landscape to a greater extent, with the Valley and Ridge classes increasingly
236 reclassified as Slope as the window size increases. This is somewhat predictable given the greater
237 spatial averaging for larger windows. However, it is the Valley class that is the most sensitive of these
238 classes over the chosen range of window sizes (**Table 1**). The Plains class is very insensitive to window
239 size. Exemplar outputs for different window size ranges are shown in **Figure 2**.

240 a) 11x11 maximum window size – this classifies the landscape features with length scales of 90-
241 330 m. This identifies much of the small-scale topography superimposed upon the major
242 ridges, hills and mountains, but provides poor characterisation of the larger-scale features.
243 For example, the valley marked with a dashed rectangle on **Figure 2a** is classified as a
244 combination of Ridge, Slope and Valley classes.

245 b) 41x41 maximum window size – this allows for the representation of features with length
246 scales between 90 m and ~1.2 km. This window size range represents both the overall
247 mountain block-scale topography as well as many of the significant Valleys (e.g. those
248 highlighted by the areas delimited by the dashed rectangle and oval in **Figure 2b**) and Passes
249 at the heads of the Valleys.

250 c) 71x71 window size – this classifies landscape features with length scales of 90 m - 2.1 km.
251 This produces a smoothed macro-scale topography, creating a ‘blocky’ characterisation of
252 the landscape with much of the meso-scale topography omitted (for example, compare the
253 area within the dashed oval in **Figure 2c with Figures 2a and 2b**).

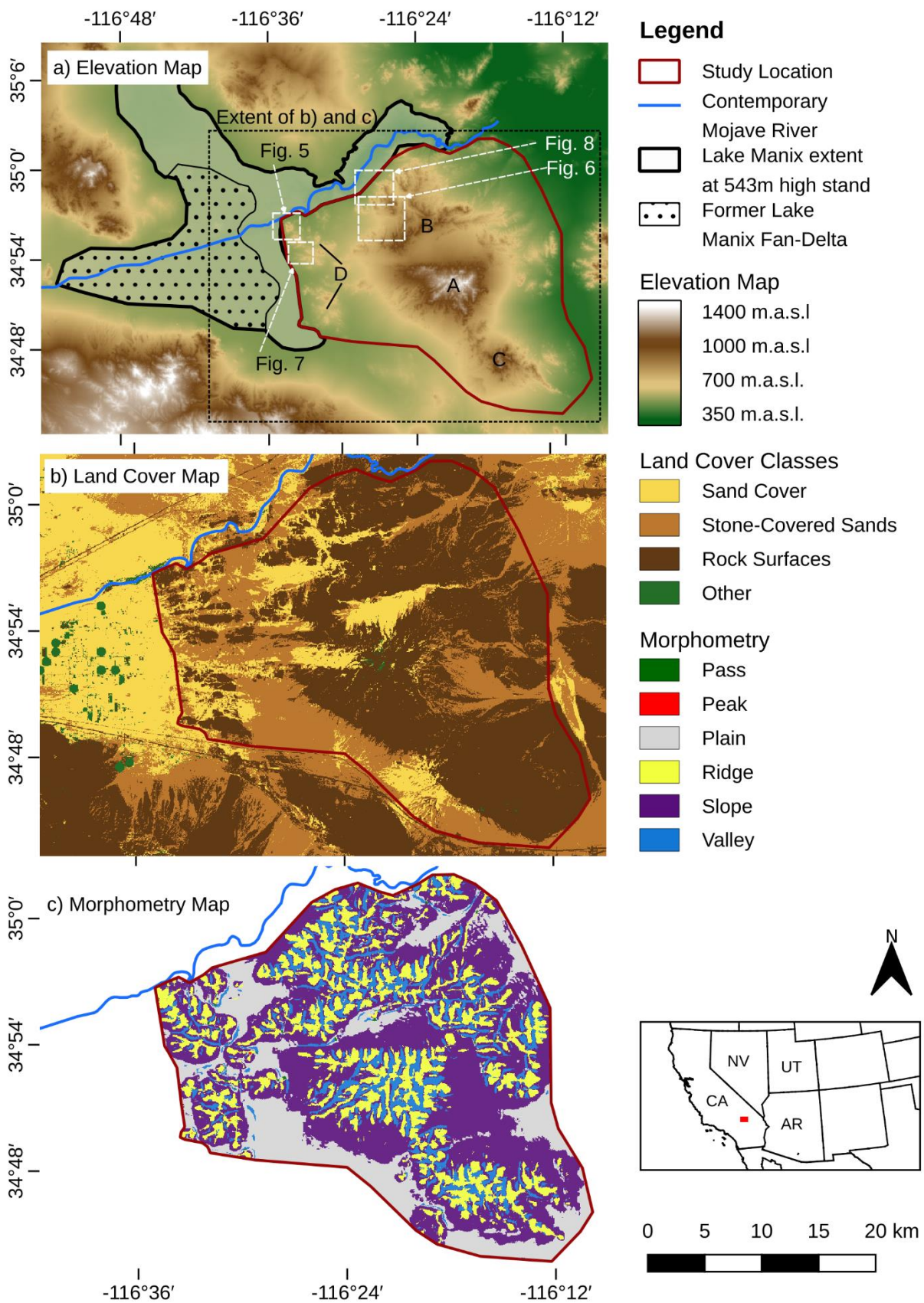
254 The 41x41 maximum window size was selected for all subsequent analyses as it most
255 appropriately maps to the largely meso-scale study focus; i.e. features with length up to
256 approximately 1.2 km. Although there are to some extent predictable changes to the LandSerf
257 output when a wider range of window sizes is utilised, at the scale of interest small changes in the
258 window size (e.g. 37x37 or 45x45 maximum window sizes) result in less than five percent variation
259 in individual pixel classifications and would not change the conclusions drawn.

260

261 **3.2 Cady Mountain land cover, elevation and morphometry**

262 **Figure 3a** shows the mountain block topography comprises a large central peak rising to 1390 m asl.
263 (Point A; **figure 3a**) with two smaller peak networks of lower altitude (about 1000 m asl.) to the
264 north and south (Points B and C in **Figure 3a**). The western margin of the mountain block comprises
265 a row of smaller (about 800 m asl.) north-south trending peaks that border the former Lake Manix
266 at 550 m asl. (Point D in **Figure 3A**) hereafter referred to as the Western Flank.

267 **Figure 3b** shows the distribution of the three land cover classes. Most of the landscape
268 comprises Rock Surfaces, with Stone-Covered Sands covering 28%, and Sand Cover representing 12%
269 of the landscape. The distribution of land cover classes is non-random (**Tables S1 to S5**). The majority
270 of pixels in the Sand Cover and Stone-Covered Sand classes lie west of 116° 18' W and north of 34°
271 50' N. Combined, they form a broadly continuous surface that encapsulates a large expanse of the
272 western half of the mountain block (**Figure 3b**). Conversely, the eastern flank of the mountain block
273 is less sandy. **Figure 3c** shows the output of the LandSerf morphometric feature classification.



274

275 **Figure 3:** (a) Elevation (b) Land cover and (c) LandSerf morphometry maps (41 x 41 pixel window size)
 276 for the Cady Mountains.

277 **3.2 Relationships between sand cover, elevation and morphometry**

278 The overall distribution of elevation varies between 388 m asl and 1390 m asl, with most of
279 the landscape located between 550 m asl and 800 m asl (**Figure 4a**). In terms of slope aspect (slopes
280 here considered generically, not in terms of the morphometric classification) there is a dominance
281 of north-facing through east-facing and southwest-facing slopes (**Figure 4b**). Most of the mountain
282 block comprises gentle slopes, with a mode of approximately 2.5° and limited areas with slope
283 gradients <1° or >6° (**Figure 4c**).

284 The proportion of the landscape in each morphometric feature class is shown in **Figure 4d**.
285 Slope is the most common morphometric class (47% of the landscape), with Plain and Ridge the
286 second and third most extensive, accounting for 20% and 19% of the landscape respectively. Peaks
287 and Passes are the least common (0.02% of the total landscape combined). The distribution of Valley
288 orientations is shown **Figure 4b**, with long axes Valleys tending to be north or east facing (i.e. 52.2%
289 combined).

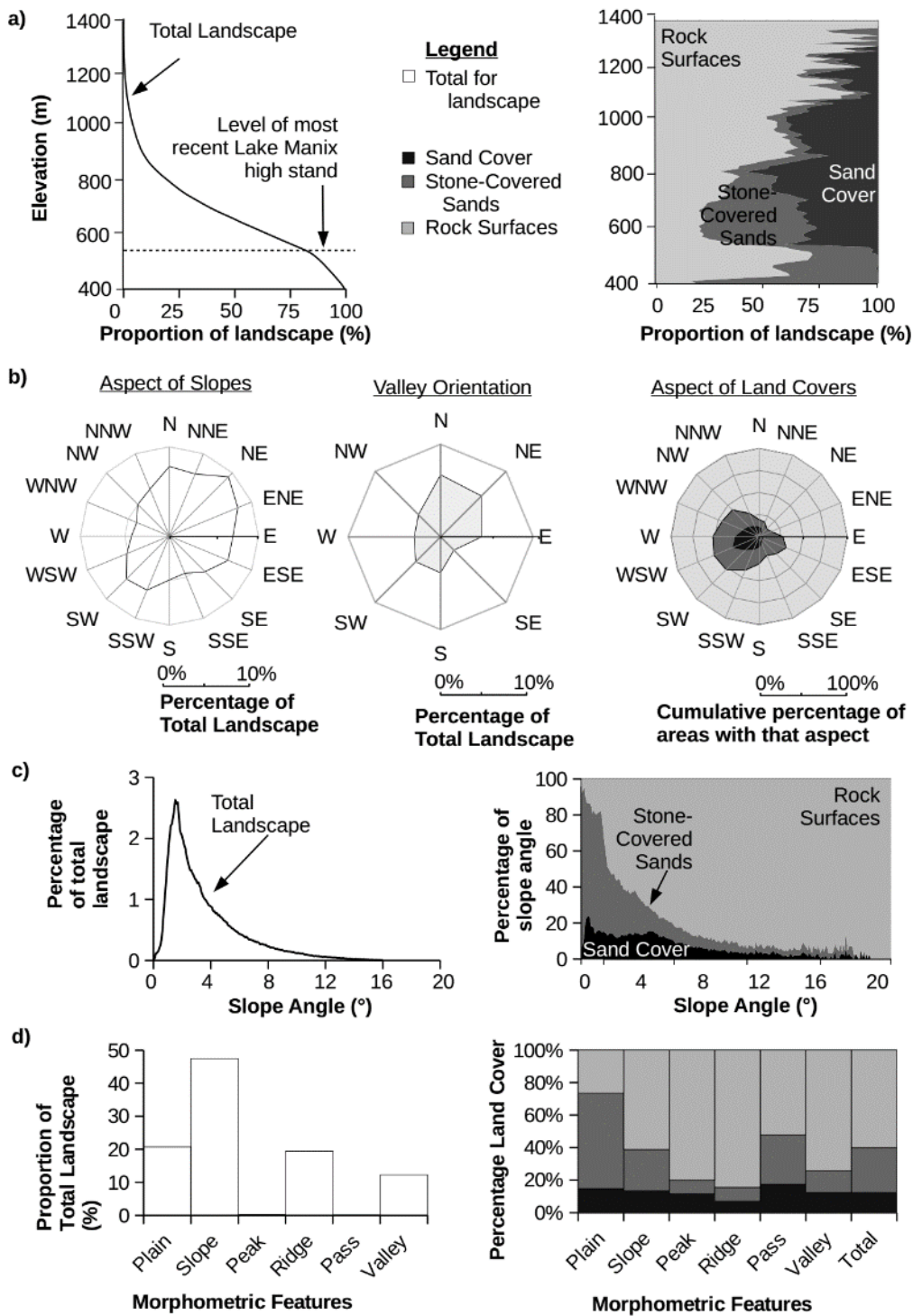
290 In terms of land cover, Sand Cover is principally located at elevations between 550 m asl. and
291 1100 m asl., where it covers 10% to 40% of the landscape, reaching its highest percentage coverage
292 by elevation (~60%) at 820 m asl (**Figure 4a**). This compares with coverages between 0% and 30%
293 above ~820 m. Stone-Covered Sand is typically found at elevations less than 800 m asl, accounting
294 for about 40% of land cover at such elevations, dropping to around 5% cover above 800 m asl. Rock
295 Surfaces are under-represented (15-35%) at intermediate elevations and dominant (>80%) above
296 1000 m asl.

297 **Figure 4b** demonstrates that Sand Cover is preferentially associated with west- and
298 southwest-facing slopes. This forms several contiguous west-facing areas in the western and central
299 portions of the mountain block (**Figures 3b and 4b**). Stone-Covered Sand has a broader aspect
300 distribution, with a mode between south-west and north-west facing slopes and another mode
301 relating to east-south-east facing slopes. Correspondingly, much of the Rock Surface class is
302 associated with north and east-facing slopes, particularly on the eastern side of the mountain block
303 (**Figure 3b and 4b**).

304 Both Sand Cover and Stone-Covered Sands are preferentially associated with low angled
305 surfaces (>80% of areas < 2° slope angle; **Figure 4c**). On surfaces between 2 and 6°, Sand Cover

306 remains at 15-20% of land cover, while Stone-Covered Sand decreases to around 20%. The Rock
307 Surface class becomes the dominant (i.e. >50%) class for surfaces steeper than 2°.

308



309

310 **Figure 4:** Summary statistics of elevation, aspect, slope angle and morphometric classes. The four
 311 rows represent (a) Elevation - showing the hypsometric curve (left) for the Cady Mountains, noting
 312 the level of the most recent Lake Manix high stand and the distribution of land cover with elevation
 313 (right) within the Cady Mountains; (b) Aspect - presenting slope aspects (for all slopes >2°(left),
 314 Valley orientations (centre) and the percentage land cover for differing slope angles (right); (c) Slope
 315 angle - presenting the distribution of slope angles (left) and the relationship between slope angle
 316 and land cover class - that is, proportion of land cover class at any given slope angle (right); (d)
 317 Morphometry - presenting the six morphometric classes in terms of total land area (left) and in terms
 318 of land cover (right). Percentages are stacked to sum to 100%.

319 Comparing against the morphometric classification (**Figure 4d**), we observe that Sand Cover
320 is approximately equally represented across the six morphometric classes (Plains (14%), Slopes
321 (13%), Passes (12%) and Valleys (12%) and Peaks (11%)), except for Ridges (7%). These values
322 compare to an overall Sand Cover of ~12% for the total landscape. Stone-Covered Sand represents
323 28% of the total landscape, but is over-represented on Plains (58%), Passes (30%) and Slopes (25%),
324 and under-represented for Valleys (13%), Ridges (8%) and Peaks (8%). Extensive Stone-Covered Sand
325 Plains are present across the western half of the mountain block and along its eastern boundary
326 (**Figures 3b and 4b**). Compared with a total Rock Surface cover of 60%, Rock Surfaces are primarily
327 represented by Ridges (84%), Peaks (80%), Valleys (74%) and on Slopes (64%) and are less
328 represented on Plains (26%). Valleys are preferentially classified as Rock Surfaces (74%; **Figure 4d**).
329 However, Valleys associated with Sand Cover and Stone-Covered Sand are observed in the northwest
330 of the Cady Mountains, and particularly in north-westerly orientated valleys (**Figure 3b**).

331 Overall, we observe that the distribution of Sand Cover with the Cady Mountains is related
332 to the landscape morphometry and aspect. Sand Cover and Stone-Covered sand are primarily
333 associated with the Plain, Slope and Pass morphometric classes, as well as NW aligned Valleys. They
334 are less associated with Ridges and Peaks and non-NW aligned Valleys. The two sand-containing land
335 cover classes are not randomly distributed (**Tables S1-S5**), and are preferentially clustered on west-
336 facing, low-angled surfaces (**Figure 4c**) across low to intermediate elevations (500-800 m asl; **figure**
337 **4a**) and are disproportionately associated (Chi-squared $p < 0.01$ in all cases; **Tables S1-S5**) with
338 Plains, Slopes and Passes (**Figure 4d and Table S4**).

339

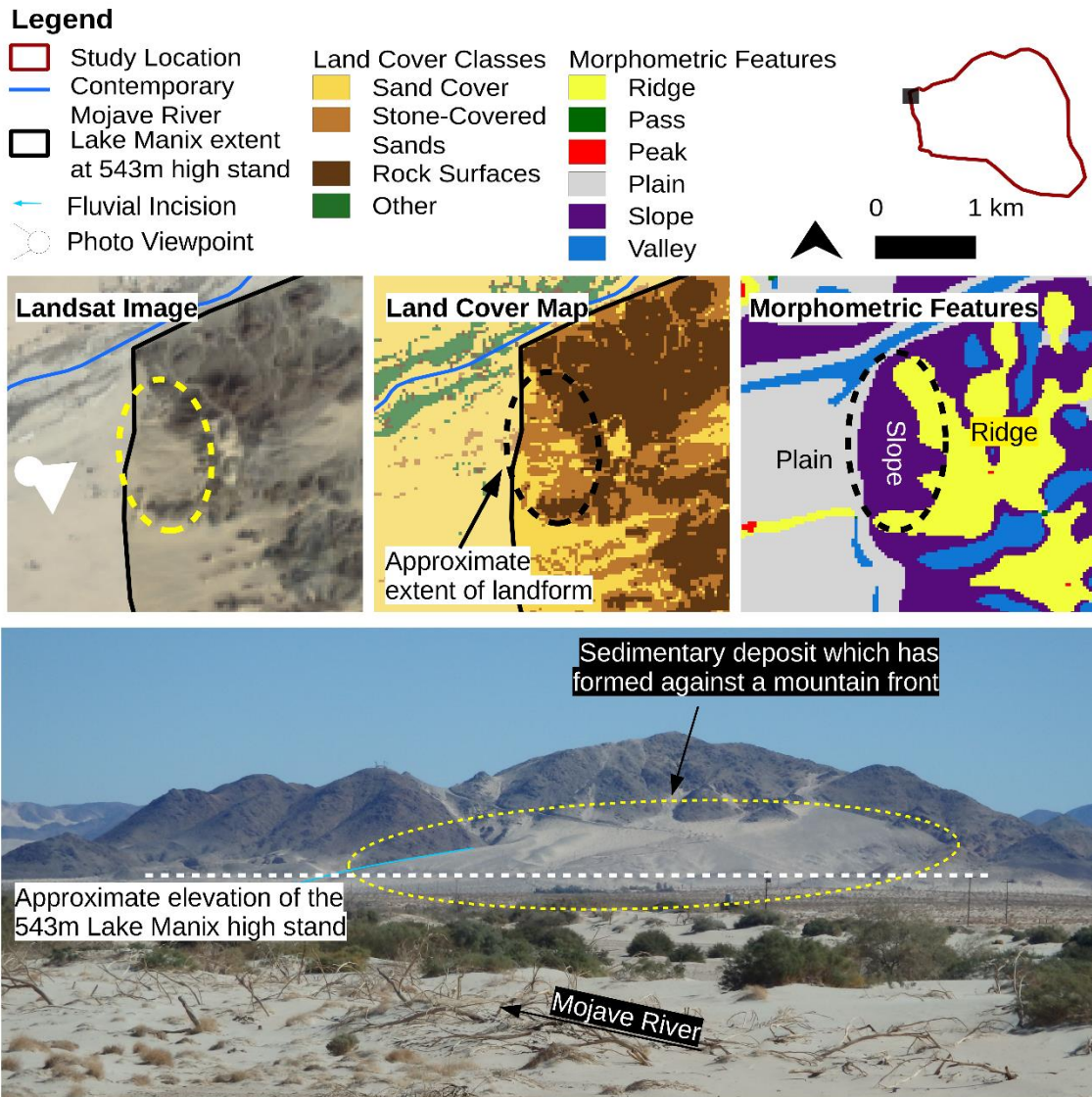
340 **3.3 Field observations**

341 This section elaborates on how the analyses of land cover and morphometry relates to field
342 observations and the character of previously described topographic dune classes.

343 **3.3.1 Slope Class**

344 A previously studied exemplar of sand accumulation within the Slope class is the Soldier Mountain
345 site (**Figure 5**), on the Western Flank of the Cady Mountain Block (Lancaster and Tchakerian, 1996).
346 Here the Slope class forms a piedmont between the Ridge (Rock Surface) to the east and a sandy
347 plain (including the Lake Manix fan delta area – not part of the morphometric analysis; **Figure 2**) to
348 the west. In detail, the LandSerf output shows the Slope and associated Sand Cover lie within an

349 embayment closely defined by the plan-form geometry of a Rock Surface Ridge (**Figure 5**). On the
 350 Slope, Sand Cover and Stone-Covered Sand form the surface materials of area approximately 0.5
 351 km², with an east-west gradient of 5-7° and a vertical range of ~130 m (**Figure 5**). Observed in the
 352 field, the Stone-Covered Sand forms a weakly developed desert pavement (Bateman *et al.*, 2012).
 353 The transition between the Sand Cover or Stone-Covered Sand Slope and the Rock Surface Ridge is
 354 marked by incisions in, notably the southern margin, which can be traced to incisions within the
 355 Ridge (**Figures 5 and S2**).



356

357 **Figure 5:** Land cover, morphometric feature class output and a ground-based image of the for sand
 358 deposits on the Slope morphometric class at Soldier Mountain. This locale represent an archetype of
 359 the Slope accommodation space type, characterised by an embayed Rock Surface Ridge (land cover
 360 and feature class respectively). The deposit itself is relatively un-dissected and is characterised by a
 361 mixture of Sand Cover and Stone-covered Sands. The elevation range from the Lake Manix high stand

362 to the upper limit of sand occurrence is ~130 m. Landsat-8 image courtesy of the U.S. Geological
363 Survey. See also **Figure S2**.

364

365 The internal composition of the Slope is clarified by a quarry to the north of the site. This
366 reveals a mixed sand, gravel and boulder composition, estimated to comprise approximately 16%
367 fluvial, debris-flow and non-aeolian sediments (Lancaster and Tchakerian, 1996; **Figure S2**). Thus, in
368 this case the Slope is formed predominantly of the aeolian sediment and compositionally is akin to
369 a sand ramp (Lancaster and Tchakerian, 1996; Bateman *et al.*, 2012). While this site lies on the
370 Western Flank of the mountain front, several comparable features lacking exposed sedimentary
371 sections can be identified within the Mountain Block itself (**Figures S6 and S7**).

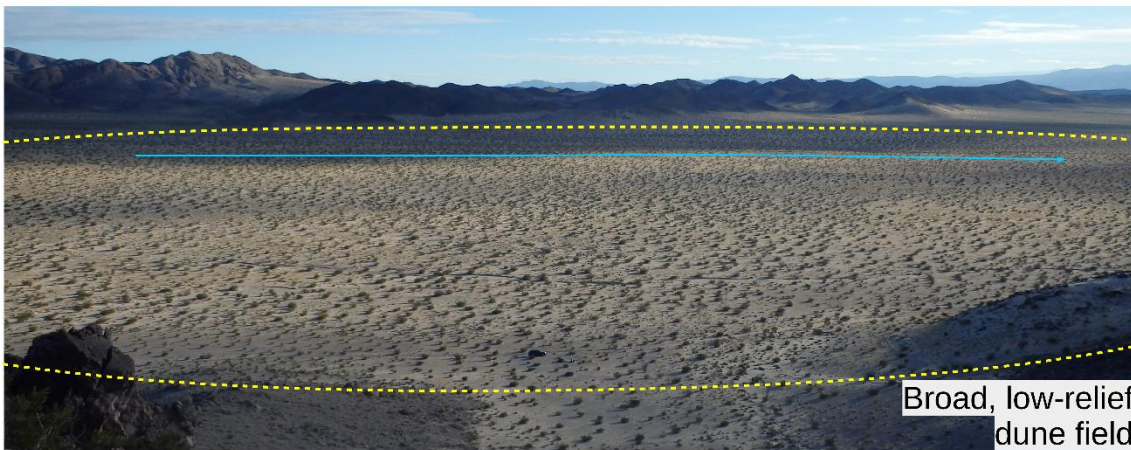
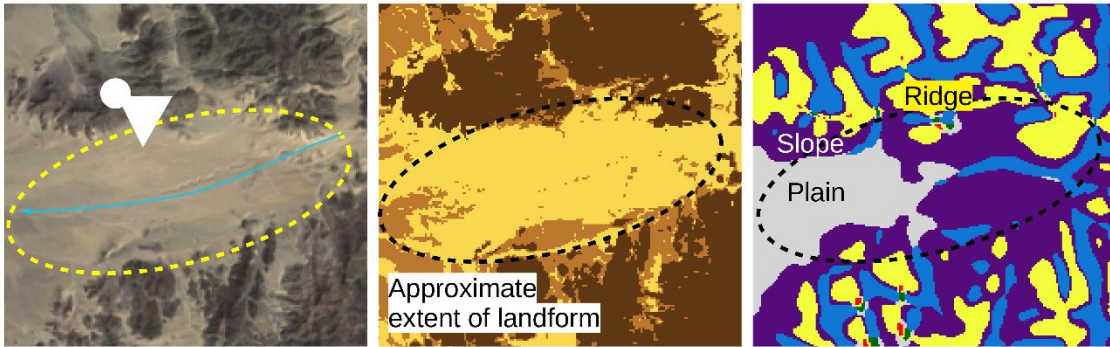
372 **3.3.2 Plains Class**

373 Extensive Sand cover associated with the Plain class is exemplified by an area about 8 km east of the
374 Western Flank (**Figure 6**). This comprises a broad, flat (<2°) Sand Plain (10 km²). Along its northerly
375 and southerly borders, the Plain class transitions to Slope and then, with increasing altitude, to
376 Ridge, with the surface cover commensurately grading from Sand Cover, to Stone-Covered Sand to
377 Rock Surface (**Figure 6**). The contemporary surface of the Sand Cover on the Plain undulates over
378 scales of < 2 m but is devoid of bedforms. At least 2.5 m of structureless sand with occasional stone
379 lines has accumulated (Hay, 2018), while the exposed roots seen for much of the shrubby (Creosote
380 Bush) vegetation attests to recent deflation (**Figure S3**).

381 In contrast to Soldier Mountain, the transition from Sand Cover to the surrounding (Rock
382 Surface) landscape is gradual. In fact, the limits of the feature (in terms of morphometry) are
383 arbitrary as the transition from Plain to Slope is defined by the 2° threshold (**Figure 6**). The limits of
384 the Plain morphometric class are not obviously morphometrically defined, but as at Soldier
385 Mountain, they are accompanied by a transition in surface materials. The transition from Sand Cover
386 to Stone-Covered Sands on the southern and western boundaries (**Figure 6**) implies contribution of
387 clasts from a steep Rock Surface sediment source. Additional examples of Sand Cover associated
388 with the Plains class are seen to the south of the example described here, and in the central Cady
389 Mountains (**Figure 3**).

390

Legend



391

392 **Figure 6:** Land cover, morphometric feature class output and a ground-based image for an exemplar
 393 of the Plains morphometric class. Here at least 2.5 m of Sand Cover has accumulated upon a broad
 394 and open Plain. The landscape is un-dissected and lacks aeolian bedforms. Note that the transition
 395 from Plain to Slope in the morphometric classification is arbitrarily defined (2°) (see text). See **also**
 396 **Figure S3**.

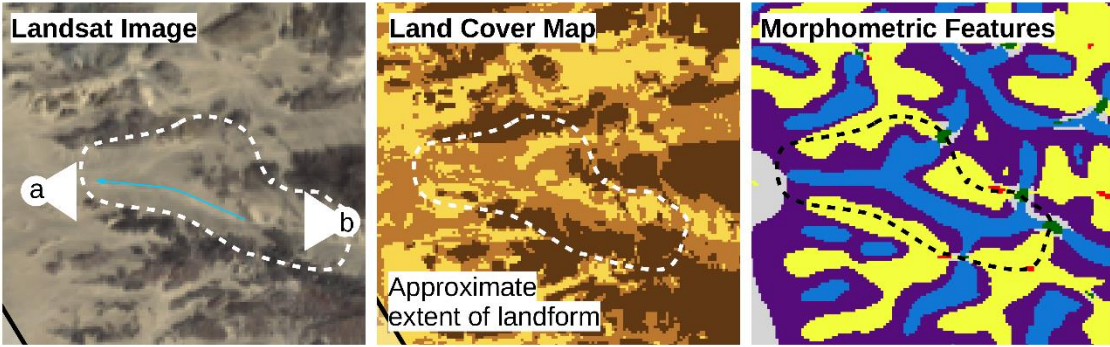
397

398 3.3.3 Valley Class

399 An example of Valley morphometric class lies along the Western Flank of the Cady Mountains,
 400 immediately south of Soldier Mountain (**Figure 7**). This represents the relatively unusual situation of
 401 significant Sand Cover within the Valley class, linked to the Pass morphometric class. The Valley has
 402 a long-axis azimuth of ~275°, is about 2 km long and 1 km wide and narrows towards two Passes at
 403 its uppermost points. The elevation ranges from 550 m asl to 700 m asl with the uppermost 50 m of
 404 the Valley associated with a Rock Surface. The Valley has a concave low-angle long axis profile (3-5°).
 405 The Valley is about 2 km², of which 1.8 km² is either Sand Cover or Stone-Covered Sands. The Sand

406 is incised along the centreline of the valley (**Figure 7**), exposing > 3 m of well-sorted medium-grained
 407 structure-less sands (largely without clasts cf. Soldier Mountain). The Valley Sand Cover is bordered
 408 on three sides by Rock Surface, although the true extent is dependent on where the western border
 409 is inferred. The highest points of the Valley adjacent to the Passes are largely devoid of sand,
 410 although the cover is varied and the transitions abrupt in places (**Figure S4**). The Pass is associated
 411 with significant quantities of W-E orientated ventifacted stones, implying transport without
 412 accumulation (Laity, 1992; **Figure 7**).

Legend



413

414 **Figure 7:** Land cover, morphometric feature class output and a ground-based images of an exemplar
415 of the Valley morphometric class. a) is a view up Valley (to the east) and b) down Valley to the west
416 with blue line showing the route of a modern channel. a) shows the Stoney Sand cover of the lower
417 valley. In b) note the Rock Surface at the top of Valley where the clasts show evidence of E-W
418 orientated ventifaction. An exposure through the Sand Cover is located in the middle left of b),
419 revealing > 3 m of structureless sands. See also **Figure S4**.

420

421 **3.3.4 Composite**

422 Field observations also identified more complex situations that illustrate the challenges of
423 this analysis approach. In these cases, we observed the close juxtaposition of the Slope and Valley
424 morphometric classes, exemplified on the northern margins of the Cady Mountains where we
425 identify the Slope-Valley composite as a locale associated with significant Sand Cover (**Figure 8**).
426 Here the Sand Cover associated Valley class emerges from the mountain block, and is partially
427 incised into a near continuous Sand and Stone-Covered Sands Slope. The Slope comprises a low-
428 angle concave Stone Covered Sand and Sand Cover surface (3 km²) extending from the mountain
429 front, decreasing in gradient from about 5° near the mountain front to around 2° at the Mojave River.
430 The Slope unit is bounded on its southern and eastern sides by the Rock Surface Ridges of the
431 mountain block, with Sand extending into five N-S orientated valleys. The break of slope between
432 the Slope unit and Rock Surface Ridges tends to be associated with Sand Cover. The Slope is incised
433 by several channels, which reveal at least 15 m of sands (**Figure S5**) interbedded with gravel and
434 sandy-gravel. The Sand Cover and Stone-Covered sand surfaces extend up the Valleys, occasionally
435 reaching a Pass. Sedimentary exposure indicates that they vary substantially in their volumetric sand
436 and gravel contents (**Figure 8 and Figure S5**).

Legend

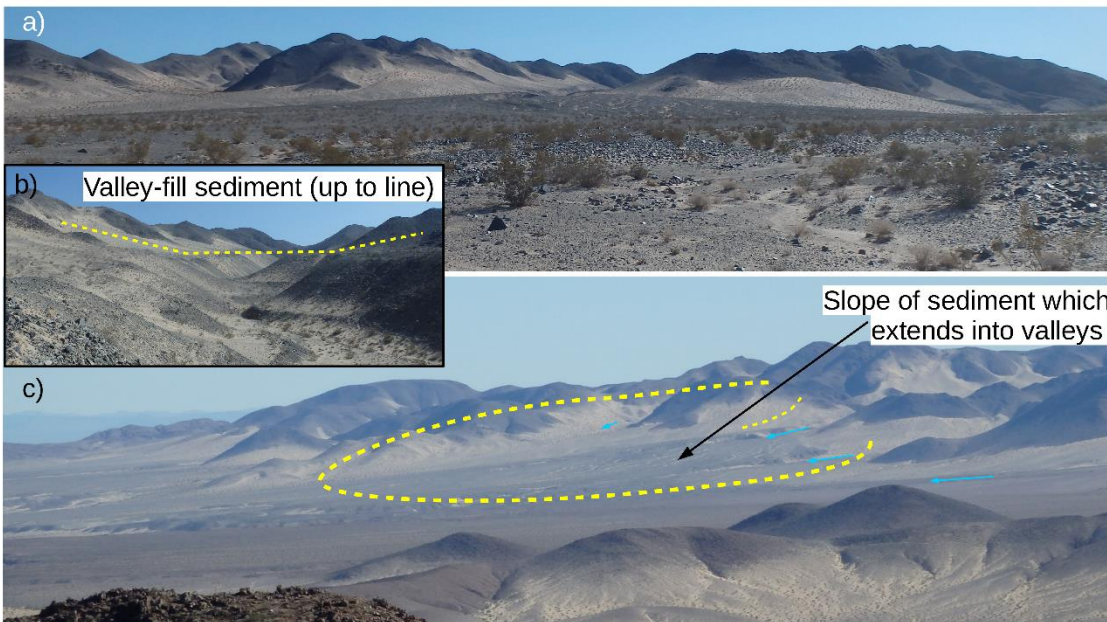
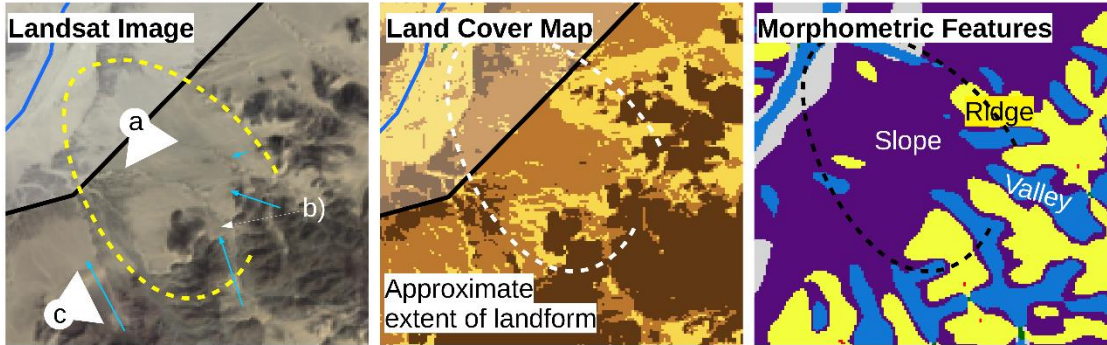
-  Study Location
-  Contemporary Mojave River
-  Lake Manix extent at 543m high stand
-  Fluvial Incision
-  Photo Viewpoint

-  Sand Cover
-  Stone-Covered Sands
-  Rock Surfaces
-  Other

-  Ridge
-  Pass
-  Peak
-  Plain
-  Slope
-  Valley



0 1 km



437

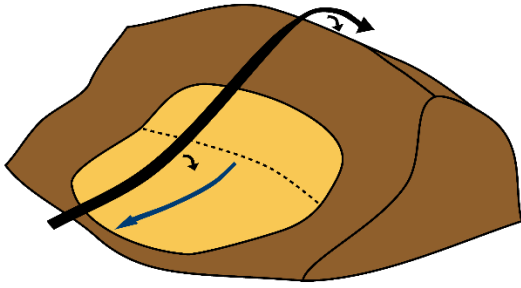
438 **Figure 8:** Land cover, morphometric feature class output and a ground-based image of an exemplar
439 of the “Slope-Valley composite” class. The Slope is dominated by Stoney Sand, which at the (limited)
440 available exposures, is seemingly typical of the overall sediment body itself (**Figure S5**). Sand and
441 Stone Covered Sand cover extend into the Valleys.

442

443 3.4 Synthesis

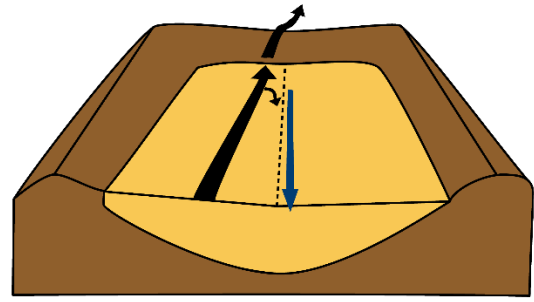
444 From these observations, and by combining the morphometry of landform surfaces and their
445 immediate topographic geometry, three zones of preferential sand accumulation within this
446 topographically complex environment are proposed. Henceforth, we refer to these as

447 *accommodation space types* (**Figure 9**). The Plain accommodation space type is defined by a flat (or
448 near-flat) Sand Cover surface without significant adjacent topography. These occur *within* the
449 mountain block in several locations (**Figure 3**); 2) The Slope accommodation space type represents
450 Sand and Stone-Covered sand that has accumulated *onto* (and partly forms) a Slope and is associated
451 particularly, but not uniquely, with the northern and western Cady Mountain margins (“the
452 Mountain Front”). Soldier Mountain falls within this class; 3) Landscapes within the Valley
453 accommodation space type are bounded by the mountain block topography (Rock Surface). These
454 largely occur on the margins of the mountain block, where Valleys (e.g. the Western Flank) alternate
455 with the Slope (class (**Figures 2 and 3**)). A fourth composite accommodation space type is
456 represented by the Slope-Valley composites that typify the northern Cady Mountain margins. In
457 total, these three individual and one composite accommodation space types account ~90% of the
458 mapped sandy landscape (i.e. 90 % of the mapped Sand and Stoney Sand cover). It should be noted
459 that in the field sand cover also clearly varies at the micro scale, from near continuous cover to
460 patchier cover, with very variable depth. This detail (e.g. **Figure S4**), which occurs over scales 10^1 m,
461 is not captured at the scale of the LandSerf analysis.



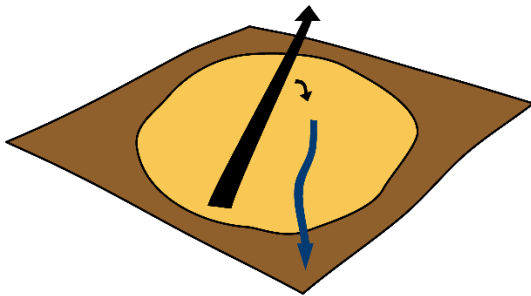
Sand ramp

Sediments accumulating on a Slope accommodation space (includes sand Ramps and likely climbing / falling dunes).



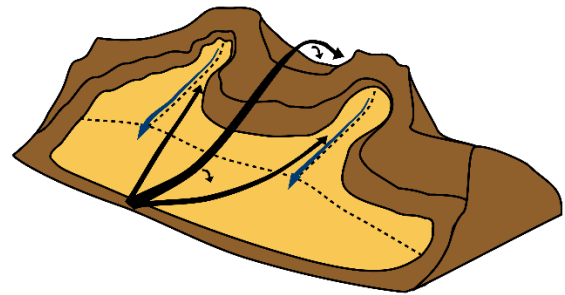
Valley-fill

Sediments accumulated within a Valley accommodation space.



Sand Sheet

Sediments accumulated within a Plain accommodation space.



Composite Landform

Sediments accumulated within (and coalescing across) multiple adjacent accommodation spaces.

Legend

- Wind Flow
- Fluvial Runoff

In this case the landform lies within two Valley and one Slope accommodation spaces

462

463 **Figure 9:** Characteristic meso-scale (lengths 10^2 - 10^3 m) accommodation space types and landforms
 464 within the Cady Mountains. The composite class manifests as a Slope-Valley composite form. This is
 465 largely associated with the northern flank of the Cady Mountains (see also **Figure 8** and **Figure S5**).

466

467 **4. Discussion**

468 Our goal was to develop a framework to consider how complex topography influences aeolian sand
 469 deposition and aeolian landform development and preservation. The combination of land cover
 470 classification, morphometric classification and field observations demonstrates that although
 471 aeolian sediment forms a broadly continuous cover across the western (windward) portion of the
 472 Cady Mountains, in relation to topography, the majority of sand-covered locales (i.e. Sand and Stone-
 473 Covered Sand) are associated with three “accommodation space types” and one composite form.

474 These account for ~90 % of Sand and Stone-Covered Sand occurrence and are depicted in **Figure 9**,
475 with the likely aeolian sediment inputs and outputs (i.e. overland flow degradation) routes indicated.
476 The next question is how such classes relate to existing aeolian landform types or classifications.

477 **4.1 Sand ramps, Climbing dunes and Falling dunes**

478 Landforms accumulating in the Slope accommodation space type are in some cases morphologically
479 and compositionally comparable to sand ramps, as exemplified by Soldier Mountain (Lancaster and
480 Tchakerian, 1996; Bateman *et al.*, 2012). Its mixed composition results from the accumulation of
481 aeolian, fluvial and sediment gravity deposits over time (Tchakerian, 1989; Bertram, 2003; Lancaster
482 and Tchakerian, 2003; see Rowell *et al.*, 2018a). The latter contribution relies on a proximal Rock
483 Surface Slope. The surface land cover also reflects this mixed composition, although free dunes can
484 be formed on these surfaces (Bateman *et al.*, 2012; Dong *et al.* 2018). Within the Cady Mountains,
485 four exemplars are identified. Two, Soldier Mountain and the East Ramp, are well defined features,
486 whose lateral extents are well (Soldier Mountain; **Figure 5**) and somewhat (East Ramp; **Figure S6**)
487 defined by surrounding Rock Surfaces and the Ridge morphometric class. Two are less defined by a
488 surrounding Rock Surface, and grade laterally to low-angle sand covered Plains (Middle Cady and
489 Cady Peak; **Figures S7 and S8**). Except for Solider Mountain these examples occur *within* the Cady
490 Mountain block, demonstrating that aeolian sediment accumulation on Slopes, and the creation of
491 sand ramp-like forms, is not exclusive to the mountain front piedmont zone, which given the
492 prevailing wind direction (W to NW), is assumed to be proximal to the primary sediment source
493 (**Section 1.2**). The restricted exposure of sediment at these interior sites (Hay, 2018) provides limited
494 insight into the relative contribution of aeolian sand versus slope material and limits our ability to
495 differentiate between climbing dunes and sand ramp (e.g. Rowell *et al.* 2018a).

496 **4.2 Sand sheets**

497 Sand sheets (Kocurek and Nielson, 1986; Warren, 2013) accumulate within the Plain accommodation
498 space type and in all cases are found *within* the wider mountain block. Each merges gradually with
499 adjacent Slopes and their boundaries are poorly defined. Of the three accommodation space types,
500 these have the highest proportion of surficial sand cover (14.8% Sand Cover and about 59% Stone
501 Covered sand). Where observed this was generally un-bedded with continuous vegetation cover.
502 These characteristics are typical of sand sheets, although some coarse-grained material is
503 incorporated as stone lines or isolated clasts (Hay, 2018). Plains are located within the mountain
504 block interior and away from piedmonts. Given the prevailing wind direction and the probable

505 sediment sources, their formation *within* the mountain block implies transfer of sand across Slope
506 (mountain front) or through Valley accommodation space types. Their extensive nature and ill-
507 defined margins reflect a gradual transition, over hundreds of metres, to steeper Slopes and a more
508 mixed sediment composition (**Figure 7**). This, and to some extent, a definition based on gradual land
509 cover change and arbitrary slope thresholds, i.e. Slope vs. Plain morphometric classes, results in
510 gradual rather than sharp transitions between areas of Sand Cover and Rock Surfaces.

511 **4.3 Valley-fill**

512 Landforms within the Valley accommodation space type are morphologically similar to Valley-Fill
513 sediments (Ellwein *et al.*, 2015). The composition of sediments within the Cady Mountain valley-fills,
514 vary from relatively stone rich (see Hay, 2018) to pure sand (**Figure S4**). In contrast to some
515 descriptions of aeolian sediment trapping by valleys (Bourke *et al.* 2014; Ellwein *et al.*, 2015), the
516 Cady examples have their long axes aligned parallel to or oblique to the prevailing sand transport
517 direction. The ventifaction seen in the Rock surfaces at their upper boundaries (Passes) shows that
518 they act both as conduits and as stores of sandy sediment.

519 **4.4 Composite**

520 The composite form represents the connection of the Slope and Valley accommodation spaces.
521 These are most clearly expressed on the northern Cady Mountains, proximal to the Mojave River,
522 and it is noteworthy that similar forms are not identified on the Western Flank of the Cady
523 Mountains, where the bedrock topography (i.e. alternating Ridges and E-W Valleys) might imply they
524 can (could have) form(ed). In terms of its morphology and expression, the northern Cady flank is
525 akin to the "sand ramp complexes" described around a complex inselberg by Bertram (2003). The
526 importance of sediment supply in filling of accommodation space and then allowing coalescence is
527 emphasised. In addition, and in contrast to the largely sandy Valley accommodation spaces on the
528 Western Flank (**Figure 7** and also Hay, 2018), the Valley-Slope composites of the northern Cady
529 Mountains are frequently composed of mixed sands and gravels. The degree of filling and extension
530 of Sand Cover into the north-south orientated Valleys (**Figure S5**) implies that at times sediment
531 supply has greatly exceeded the Valley catchments' capacity to evacuate sediment. Such forms are
532 found primarily in the areas closest to Mojave River, which presumably represents an upwind
533 sediment source. In conjunction with their apparent incision under modern conditions (**Figure S5**)

534 the stacked sequences of sand, mixed sand gravel, and gravel within the Slope unit imply a long and
535 complex history of sediment filling and evacuation.

536

537 **4.5 Implications**

538 Although the Cady Mountain block is a topographically complex area, this analysis suggests that four
539 broad types of accommodation spaces are associated with the majority of the remotely sensed Sand
540 Cover and Stoney Sand Cover. This provides a framework with which to consider the preserved
541 aeolian record in this region. Some accommodation spaces have clearly delimited boundaries. The
542 Soldier Mountain sand ramp is an exemplar, with an arcuate planform determined by a Rock Surface
543 Ridge. Similarly, many previously described sand ramps occur against isolated inselbergs (Rowell *et*
544 *al.*, 2018a). However, Soldier Mountain and to a lesser extent the Eastern Ramp (ER; **Figure S6**), are
545 largely the exception within the Cady Mountains. By contrast, Sand Cover, and by inference, aeolian
546 sedimentation history, is represented by a semi-continuous patchwork of accommodation space
547 types. This reflects the coalescence of deposits that are initially associated with discrete
548 accommodation spaces, exemplified today on the northern Cady Mountain margin. Four factors may
549 influence this: 1) the proximity of underlying accommodation spaces to one another (geological
550 control); 2) subtle or gradual changes in underlying topography (e.g. the Plain to Slope transition);
551 3) variation in, or proximity to, a sediment supply; 4) the preservation of sediment once within
552 spaces.

553 Considering temporal aspects, it is assumed that accommodation spaces fill or degrade as
554 the balance between sand supply and erosive capacity fluctuates. Thus, an accumulation may
555 coalesce or divide as it grows and degrades. Progressive filling of low points has been observed, in a
556 more subtle manner, associated with debris flow levees on steep coastal slopes in the Atacama
557 Desert (Ventra *et al.*, 2017). Substituting space (distance from sediment source) for time, Ellwein *et*
558 *al.* (2015) also argued that valley fill aeolian deposits develop through progressive space-filling,
559 whereby sand accumulates within topographic lows, increasingly masking smaller-scale topography
560 and non-aeolian deposits in the process. This potentially enhances preservation potential as the land
561 surface becomes sandier and more permeable. Comparable processes are operating in the Valley
562 and Plain accommodation spaces within the Cady Mountains.

563 Ventra *et al.* (2017) argued that local-scale topographic control via the generation of surface
564 run off is critical in controlling the long-term accumulation and preservation of topographic dune
565 forms. Presently available dating for the Soldier Mountain sand ramp demonstrates the preservation
566 timescale for sands within the Slope accommodation space type is of the order 10^4 years (note
567 contrasting age estimates; Rendell and Sheffer, 1996; Bateman *et al.* 2012). However, evidence for
568 incision of the existing deposits, particularly in the case of the Slope and Slope-Valley composite,
569 under modern conditions is clearly identified (**Figures 5, 7 and 8**).

570 In this sense, we can also consider the character and drivers of the Cady Mountain aeolian
571 sedimentary records within different accommodation spaces as, for example, one might seek to infer
572 via a programme of luminescence dating. For example, the Plains accommodation space is, in all
573 cases, distal to the assumed sediment source. In general, sand sheets tend to be associated with
574 several factors, including a high water-table, periodic flooding, and the presence of vegetation
575 (Kocurek and Nielson, 1986). Despite the relatively slow accumulation of aeolian sediment on a
576 vegetated surface that is implied, in this context, preservation potential may be higher than Slope
577 and Valley contexts as the accommodation space is more distant from areas of concentrated surface
578 runoff. Conversely, in lacking significant stone cover these sands – via changing vegetation cover (e.g.
579 Forman *et al.* 2006; Chase and Thomas, 2007) – are potentially more sensitive to reworking due to
580 climatic perturbations (assuming no change in upwind sediment supply). Indeed, Ellwein *et al.*
581 (2011; 2015) reported distinct suites of OSL ages for topographic dunes compared to sand sheets at
582 Black Mesa, Arizona, with the latter inferred to represent the timing of sand stabilisation with soil
583 development.

584 In the Slope and Valley accommodation space types the sediment source is more (e.g. Soldier
585 Mountain) or less (East Ramp) proximal and in the case of the former, accumulation rates were
586 potentially high (Bateman *et al.* 2012, but cf. Rendell and Sheffer, 1996). However, accumulation
587 rates and deposit thickness are challenging to compare as the Slope and Valley accommodation
588 spaces will almost certainly include contributions of talus from Rock Surfaces (Bateman *et al.*, 2012).
589 More generally, any tendency for accumulation in such contexts is tempered by the preservation-
590 limiting factor of the surrounding Rock Surfaces, which readily generate overland flow, which will
591 also respond to climatic changes. Thus, the controls on the accumulation and erosion balance in
592 such contexts are potentially subtle and site specific (Ventra *et al.*, 2017). Both Soldier Mountain and

593 the composite Slope-Valley fills on the northern Cady Mountains margin are cut by well-developed
594 channels, which are tied to major (geologically controlled) Valley forms.

595 Overall, we propose that the preserved aeolian sedimentary record, driven by fluctuations in
596 sediment supply, availability and transport capacity will be further mediated by meso-scale
597 topographic controls. This reflects the fact that the morphometric analysis suggests a large
598 proportion of sand cover is associated with four meso-scale topographic contexts. The identified
599 accommodation space types may be more or less sensitive to event-based accumulation and
600 erosion, e.g. Slopes, or to secular changes in climatic conditions, e.g. Plains, both of which will
601 generate characteristic “residence times” for sand in different contexts. There is potential to test
602 such inferences by combining luminescence dating chronologies, regional palaeoclimatic
603 information and the morphometric analyses presented here, although an obvious corollary is that a
604 limited suite of luminescence ages would be very challenging to interpret.

605 A challenge to the approach outlined here is the use of a DEM based on the modern land
606 surface, which includes the accumulated sand. In almost all instances, there is a weakly constrained
607 thickness of sediment fill and uncertainty in the volume of the accommodation space(s). Although
608 there is an absence of sedimentary exposure in most cases, the fill exceeds 25 m at Soldier Mountain,
609 and 15 m on the northern margins of the Cady Mountains (**Figure S5**). The degree to which this is an
610 impediment to this mapping approach is probably site dependent. In the Cady Mountains the relief
611 of the mountain block is far greater than that of most exposed aeolian deposits, and it is likely that
612 the large-scale shape of the underlying topography is reasonably well represented by the DEM.
613 Quantities of aeolian sediment sufficient to alter the morphometry are focused on piedmonts. At
614 these locales, notably the northern and western margins of the Cady Mountains, it is likely that the
615 contemporary surface of any aeolian deposits obscures the bedrock topography, leading to an
616 increase in the proportion of landscape morphometrically classified as Slope. The interpretation of
617 such areas therefore needs to be supported by field observation.

618 **5. Conclusions**

619 Based on a combination of land cover mapping and morphometric analysis, we sought to
620 characterise the patterns of aeolian sediment accumulation across an area of complex topography.
621 From this we show that despite a high-relief topographically complex setting, aeolian deposits are
622 primarily associated with three morphometric classes (and hence accommodation space types);

623 Slope, Plain and Valley and one composite (Slope-Valley) class. Together these account for ~90% of
624 the mapped sand cover in the study area. These broadly map to or include recognised aeolian
625 landforms, such as sand ramps, sand sheets and valley-fills. However, most accommodation spaces
626 lack distinct boundaries and where sediment supply is high composite forms develop. Whether such
627 coalescence occurs is likely to depend upon the association of different accommodation space types
628 (controlled by the form of the underlying bedrock) and the progressive filling of the accommodation
629 spaces, which will be time-bounded.

630 Overall, we show that meso-scale topography is a clear control on the character of aeolian
631 sediment accumulation in the Cady Mountains. Topography will mediate the residence time or
632 climatic sensitivity of the aeolian sedimentary record through its impact on: 1) sediment storage
633 volume, 2) potential for erosion via runoff, 3) preservation moderated via vegetation vs. moderate
634 stone coverage and 4) sediment supply (nature of, and distance to, character of intervening
635 topography). We hypothesise that these may generate differences in the preserved aeolian
636 chronostratigraphic records between sites. In this instance, the most obvious differences are likely
637 to be between downwind sand sheet deposits and upwind, more strongly Rock Surface-influenced,
638 Slope (Mountain Front) and Valley Fill contexts.

639

640 **Acknowledgements**

641 ASH was supported by NERC studentship 1358108. Rob Fulton, Jason Wallace and Simon Benson
642 are thanked for logistical support. Three reviewers and the editor are thanked for their
643 constructive comments on an earlier version of this paper.

644

645 **References**

646 Bateman, M.D., Bryant, R.G., Foster, I.D.L., Livingstone, I., Parsons, A.J. 2012. On the formation of
647 sand ramps: A case study from the Mojave Desert. *Geomorphology* **161–162**, 93–109.

648 Bertram S. 2003. Late Quaternary sand ramps in south-western Namibia-Nature, origin and
649 palaeoclimatological significance, Doctoral Thesis, University of Würzburg: Würzburg, Germany

- 650 Blaney, H.F. 1957. Evaporation study at Silver Lake in the Mojave Desert, California. *Eos, Transactions*
651 *American Geophysical Union* **38**, 209-215.
- 652 Bourke, M.C., Bullard, J.E. Barnouin-Jha, O.S., 2004. Aeolian sediment transport pathways and
653 aerodynamics at troughs on Mars. *Journal of Geophysical Research: Planets*, **109**(E7).
- 654 Bullard, J.E., Nash, D.J. 2000. Valley-marginal sand dunes in the south-west Kalahari: their nature,
655 classification and possible origins. *Journal of Arid Environments* **45**, 369–383.
- 656 Chase, B.M., Thomas, D.S.G., 2007. Late Quaternary dune accumulation along the western margin
657 of South Africa: distinguishing forcing mechanisms through the analysis of migratory dune forms.
658 *Earth and Planetary Science Letters* **251**, 318-333
- 659 Clarke, M.L., Rendell, H.M. 1998. Climate change impacts on sand supply and the formation of desert
660 sand dunes in the south-west U.S.A. *Journal of Arid Environments* **39**, 517–531.
- 661 Clemmensen, L.B., Fornós, J.J., Rodriguez-Perea, A. 1997. Morphology and architecture of a late
662 Pleistocene cliff-front dune, Mallorca, Western Mediterranean. *Terra Nova* **9**, 251-254
- 663 Dong, M., Yan, P., Liu, B., Wu, W., Meng, X., Ji, X., Wang, Y. Wang, Y., 2018. Distribution patterns and
664 morphological classification of climbing dunes in the Qinghai-Tibet Plateau. *Aeolian Research* **35**, 58-
665 68.
- 666 Drăguț, L. Eisank, C. 2011. Object representations at multiple scales from digital elevation models.
667 *Geomorphology* **129**, 183-189.
- 668 Ellwein, A.M., Mahan, S.A., McFadden, L.D. 2011. New optically stimulated luminescence ages
669 provide evidence of MIS3 and MIS2 eolian activity on Black Mesa, northeastern Arizona, USA.
670 *Quaternary Research* **75**, 395-398
- 671 Ellwein, A.L., Mahan, S.A., McFadden, L.D. 2015. Impacts of climate change on the formation and
672 stability of late Quaternary sand sheets and falling dunes, Black Mesa region, southern Colorado
673 Plateau, USA. *Quaternary International* **362**, 87–107.
- 674 Enzel, Y. 1992. Flood frequency of the Mojave River and the formation of late Holocene playa lakes,
675 southern California, USA. *The Holocene* **2**, 11-18.

- 676 Enzel, Y., Wells, S.G., Lancaster, N. 2003. Late Pleistocene lakes along the Mojave River, southeast
677 California. In: *Paleoenvironments and paleohydrology of the Mojave and southern Great Basin*
678 *deserts*. Geological Society of America Special Paper **368**, 61–77
- 679 Evans, J.R. 1962. Falling and Climbing Sand Dunes in the Cronese (“Cat”) Mountain Area, San
680 Bernardino County, California. *The Journal of Geology* **70**, 107-113
- 681 Fisher, P., Wood, J., Cheng, T. 2004. Where is Helvellyn? Fuzziness of multi-scale landscape
682 morphometry. *Transactions of the Institute of British Geographers* **29**, 106–128.
- 683 Forman, S.L., Spaeth, M., Marín, L., Pierson, J., Gómez, J., Bunch, F. Valdez, A., 2006. Episodic Late
684 Holocene dune movements on the sand-sheet area, Great Sand Dunes National Park and Preserve,
685 San Luis Valley, Colorado, USA. *Quaternary Research* **66**, 97-108.
- 686 Garvey, B., Castro, I.P., Wiggs, G.F.S., Bullard, J.E. 2005. Measurements of Flows Over Isolated Valleys.
687 *Boundary-Layer Meteorology* **117**, 417–446.
- 688 Hay, A.S. 2018. *The Influence of Complex Topography on Aeolian Sediment Accumulation and*
689 *Preservation: An Investigation of Morphology and Process History*, Unpublished PhD Thesis,
690 University of Leicester.
- 691 Hesse P. 2019. Sand Seas. In: Livingstone, I., Warren, A. (eds). *Aeolian geomorphology: A New*
692 *Introduction*. Wiley, 179–208.
- 693 Howard AD. 1985. Interaction of sand transport with topography and local winds in the north
694 Peruvian coastal desert. In *Proceedings of International Workshop on the Physics of Blown*,
695 *Barndorff-Nielsen OE (ed)*. University of Aarhus: Aarhus, Denmark; 511–544.
- 696 Khiry MA. 2007. *Spectral mixture analysis for monitoring and mapping desertification processes in*
697 *semi-arid areas in North Kordofan State, Sudan*, Doctor of Natural Science, Technische Universität
698 Dresden: Dresden, Germany
- 699 Kocurek G, Lancaster N. 1999. Aeolian system sediment state: theory and Mojave Desert Kelso dune
700 field example. *Sedimentology* **46**, 505–515.

- 701 Kocurek G, Nielson J. 1986. Conditions favourable for the formation of warm-climate aeolian sand
702 sheets. *Sedimentology* **33**, 795–816.
- 703 Kumar A, Srivastava P, Meena NK. 2017. Late Pleistocene aeolian activity in the cold desert of Ladakh:
704 A record from sand ramps. *Quaternary International* **443**, 13–28.
- 705 Laity J.E. 1992. Ventifact evidence for Holocene wind patterns in the east-central Mojave Desert.
706 *Zeitschrift fur Geomorphologie* **84**, 73–88.
- 707 Lancaster N. 1994. Controls on aeolian activity: some new perspectives from the Kelso Dunes,
708 Mojave Desert, California. *Journal of Arid Environments* **27**, 113–125.
- 709 Lancaster N, Tchakerian V.P. 1996. Geomorphology and sediments of sand ramps in the Mojave
710 Desert. *Geomorphology* **17**, 151–165.
- 711 Lancaster N, Tchakerian V.P. 2003. Late Quaternary eolian dynamics, Mojave Desert, California. In:
712 Paleoenvironments and paleohydrology of the Mojave and southern Great Basin deserts. Geological
713 Society of America Special Paper **368**, 231–249
- 714 Lui, X., Li, S., Shen, J., 1999. Wind tunnel simulation experiment of mountain dunes. *Journal of Arid*
715 *Environments* **42**, 49-59.
- 716 Meek, N. 1989. Geomorphic and hydrologic implications of the rapid incision of Afton Canyon,
717 Mojave Desert, California. *Geology* **17**, 7-10.
- 718 Miliareisis G. Ch. 2001. Extraction of bajadas from digital elevation models and satellite imagery.
719 *Computers & Geosciences* **27**, 1157–1167.
- 720 Muhs D.R., Lancaster N, Skipp G.L. 2017. A complex origin for the Kelso Dunes, Mojave National
721 Preserve, California, USA: A case study using a simple geochemical method with global applications.
722 *Geomorphology* **276**, 222–243.
- 723 Norini, G., Zuluaga M.C., Ortiz, I.J., Aquino, D.T., Lagmay, A.M.F. 2016. Delineation of alluvial fans
724 from Digital Elevation Models with a GIS algorithm for the geomorphological mapping of the Earth
725 and Mars. *Geomorphology* **273**, 134–149.

- 726 Paichoon, M.S., 2020. Analysis of the origin, formation and development of sand ramps on the
727 Eastern slopes of Shirkouh, Yazd, Central Iran. *Geomorphology* **351**, 106891.
- 728 Pease, P.P., Tchakerian, V.P. 2003. Geochemistry of sediments from Quaternary sand ramps in the
729 southeastern Mojave Desert, California. *Quaternary International* **104**, 19–29.
- 730 Qian, G., Dong, Z., Luo, W. Lu, J. 2011. Mean airflow patterns upwind of topographic obstacles and
731 their implications for the formation of echo dunes: A wind tunnel simulation of the effects of
732 windward slope. *Journal of Geophysical Research*, **116**
- 733 Ramsey, M.S., Christensen, P.R., Lancaster, N., Howard, D.A. 1999. Identification of sand sources and
734 transport pathways at the Kelso Dunes, California, using thermal infrared remote sensing. *Geological*
735 *Society of America Bulletin* **111**, 646–662.
- 736 Reheis, M.C., Redwine, J.L. 2008. Lake Manix shorelines and Afton Canyon terraces: Implications for
737 incision of Afton Canyon. In: *Late Cenozoic Drainage History of the Southwestern Great Basin and*
738 *Lower Colorado River Region: Geologic and Biotic Perspectives*. Geological Society of America Special
739 Paper **439**, 227–259.
- 740 Rendell, H.M., Sheffer, N.L. 1996. Luminescence dating of sand ramps in the Eastern Mojave Desert.
741 *Geomorphology* **17**, 187-197.
- 742 Rowell, A., Thomas D.S., Bailey, R.M., Stone, A, Garzanti, E., Padoan, M. 2018a. Controls on sand
743 ramp formation in southern Namibia. *Earth Surface Processes and Landforms* **43**, 150–171.
- 744 Rowell, A.L., Thomas, D.S., Bailey, R.M. Holmes, P.J., 2018b. Sand ramps as palaeoenvironmental
745 archives: Integrating general principles and regional contexts through reanalysis of the Klipkraal
746 Sands, South Africa. *Geomorphology* **311**, 103-113.
- 747 Schaetzl, R.J., Larson, P.H., Faulkner, D.J., Running, G.L., Jol, H.M. Rittenour, T.M. 2018. Eolian sand
748 and loess deposits indicate west-northwest paleowinds during the Late Pleistocene in western
749 Wisconsin, USA. *Quaternary Research* **89**, 769-785.
- 750 Smith, R.S.U. 1984. Eolian geomorphology of the Devils Playground, Kelso Dunes and Silurian Valley,
751 California. *Western Geological Excursions*. Vol. 1: Geological Society of America 97th Annual Meeting
752 Field Trip Guidebook, Reno, Nevada, 239–251.

- 753 Tchakerian, V.P. 1991. Late Quaternary Aeolian Geomorphology of the Dale Lake Sand Sheet,
754 Southern Mojave Desert, California. *Physical Geography* **12**, 347–369.
- 755 Telfer, M.W., Mills, S.C., Mather, A.E. 2014. Extensive Quaternary aeolian deposits in the Drakensberg
756 foothills, Rooiberge, South Africa. *Geomorphology* **219**, 161–175.
- 757 Tsoar, H. 1983. Wind Tunnel Modeling of Echo and Climbing Dunes. In: Brookfield ME and Ahlbrandt
758 TS (eds). *Developments in Sedimentology*, Elsevier, 247–259.
- 759 del Valle, L., Gomez-Pujol, L., Fornos, J.J., Timar-Gabor, A., Anechiteie-Deacu V., Pomar, F. 2016.
760 Middle to Late Pleistocene dunefields in rocky coast settings at Cala Xuclar (Eivissa, Western
761 Mediterranean): Recognition, architecture and luminescence chronology. *Quaternary International*
762 407, 4-13
- 763 Ventra, D, Rodríguez-López, J.P., de Boer, P.L. 2017. Sedimentology and preservation of aeolian
764 sediments on steep terrains: Incipient sand ramps on the Atacama coast (northern Chile).
765 *Geomorphology* **285**, 162–185.
- 766 Warren A. 2013. *Dunes: Dynamics, Morphology, History*. Wiley-Blackwell, 236pp
- 767 Wells, S.G., Brown, W.J., Enzel, Y., Anderson, R.Y., McFadden, L.D., 2003. Late Quaternary geology
768 and paleohydrology of pluvial Lake Mojave, southern California. *Geological Society of America*
769 *Special Paper* 358, 79–114.
- 770 White, B.R., Tsoar, H. 1998. Slope effect on saltation over a climbing sand dune. *Geomorphology* **22**,
771 159–180.
- 772 Wilson, I.G. 1973. *Ergs*. *Sedimentary Geology* **10**, 77-106
- 773 Wood, J. 1996. *The Geomorphological Characterisation of Digital Elevation Models*, PhD, University
774 of Leicester.
- 775 Wood, J. 2009a. Geomorphometry in LandSerf. In Hengl T and Reuter HI (eds). *Developments in Soil*
776 *Science*. Elsevier; 333–349.
- 777 Wood, J. 2009b. *The landserf manual. User Guide for LandSerf*, 23.
778 <http://www.staff.city.ac.uk/~jwo/landserf/landserf230/doc/landserfManual.pdf> Xiao, J., Qu, J., Yao,

779 Z., Pang, Y., Zhang, K. 2015. Morphology and formation mechanism of sand shadow dunes on the
780 Qinghai-Tibet Plateau. *Journal of Arid Lands* **7**, 10–26.

781 Zimbelman, J.R., Williams, S.H., Tchakerian, V.P. 1995. Sand Transport Paths. In: Tchakerian V.P. (ed).
782 Desert Aeolian Processes, Chapman & Hall: London.

783

784 **Figure Captions**

785 **Figure 1:** Location map and satellite image for the Cady Mountains, within the southwest USA,
786 showing the location of the Cady Mountain Block in relation to the Mojave River, palaeo-Lake Manix,
787 Soda and Silver Lakes, which in the past formed palaeo-Lake Mojave, as well as Harper Lake Basin.
788 Also shown is the approximate location of the Lake Manix fan delta, a putative source for the Cady
789 Mountains aeolian deposits.

790 **Figure 2:** Outputs of the LandSerf analyses of the Cady Mountains presented as southeast looking
791 oblique views of the northwest of the Cady Mountain Block. The three panes (a-c) show the
792 morphometric classification for the same portion of landscape at three examples of analysis scales
793 (i.e. different maximum window size ranges): a) 3x3 to 11x11 pixels; b) 3x3 to 41x41 pixels; 3x3 to
794 71x71 pixels. Each pixel in image the represents the most common morphometric class at the range
795 of scales considered. The legend illustrates the six morphometric classes. The lower right-hand
796 image shows the direction of view with an image of the study area, with the Mojave River in blue
797 and the Western Flank of Cady Mountains shown in red.

798 **Figure 3:** (a) Elevation (b) Land cover and (c) LandSerf morphometry maps (41 x 41 pixel window
799 size) for the Cady Mountains.

800 **Figure 4:** Summary statistics of elevation, aspect, slope angle and morphometric classes. The four
801 rows represent (a) Elevation - showing the hypsometric curve (left) for the Cady Mountains, noting
802 the level of the most recent Lake Manix high stand and the distribution of land cover with elevation
803 (right) within the Cady Mountains; (b) Aspect - presenting slope aspects (for all slopes $>2^\circ$ (left),
804 Valley orientations (centre) and the percentage land cover for differing slope angles (right); (c) Slope
805 angle - presenting the distribution of slope angles (left) and the relationship between slope angle
806 and land cover class - that is, proportion of land cover class at any given slope angle (right); (d)

807 Morphometry - presenting the six morphometric classes in terms of total land area (left) and in
808 terms of land cover (right). Percentages are stacked to sum to 100%.

809 **Figure 5:** Land cover, morphometric feature class output and a ground-based image of the for sand
810 deposits on the Slope morphometric class at Soldier Mountain. This locale represent an archetype
811 of the Slope accommodation space type, characterised by an embayed Rock Surface Ridge (land
812 cover and feature class respectively). The deposit itself is relatively un-dissected and is characterised
813 by a mixture of Sand Cover and Stone-covered Sands. The elevation range from the Lake Manix high
814 stand to the upper limit of sand occurrence is ~130 m. Landsat-8 image courtesy of the U.S.
815 Geological Survey. See also Figure S2.

816 **Figure 6:** Land cover, morphometric feature class output and a ground-based image for an exemplar
817 of the Plains morphometric class. Here at least 2.5 m of Sand Cover has accumulated upon a broad
818 and open Plain. The landscape is un-dissected and lacks aeolian bedforms. Note that the transition
819 from Plain to Slope in the morphometric classification is arbitrarily defined (2°) (see text). See also
820 Figure S3.

821 **Figure 7:** Land cover, morphometric feature class output and a ground-based images of an exemplar
822 of the Valley accommodation space type. a) is a view up Valley (to the east) and b) down Valley to
823 the west with blue line showing the route of a modern channel. a) shows the Stoney Sand cover of
824 the lower valley. In b) note the Rock Surface at the top of valley where the clasts show evidence of
825 E-W orientated ventifaction. An exposure through the Sand Cover is located in the middle left of b),
826 revealing > 3 m of structureless sands. See also Figure S4.

827 **Figure 8:** Land cover, morphometric feature class output and a ground-based image of an exemplar
828 of the "Slope-Valley composite" class. The Slope is dominated by Stoney Sand, which at the (limited)
829 available exposures, is seemingly typical of the overall sediment body itself (Figure S5). Sand and
830 Stone Covered Sand cover extend into the Valleys.

831 **Figure 9:** Characteristic meso-scale (lengths 102-103 m) accommodation space types and landforms
832 within the Cady Mountains. The composite class manifests as a Slope-Valley composite form. This is
833 largely associated with the northern flank of the Cady Mountains (see also Figure 8 and Figure S5)..

834 Tables

835 **Table 1:** The effect of Landsat window size morphometric classification outputs (as percentages of
836 the total land surface)